Human Molecular Genetics, 2016, Vol. 25, No. 8 1489–1500

doi: 10.1093/hmg/ddw026
Advance Access Publication Date: 1 February 2016
Original Article

ORIGINAL ARTICLE

Glycosylation abnormalities in Gdt1p/TMEM165 deficient cells result from a defect in Golgi manganese homeostasis

Sven Potelle[1], Willy Morelle[1], Eudoxie Dulary[1], Sandrine Duvet[1], Dorothée Vicogne[1], Corentin Spriet[1], Marie-Ange Krzewinski-Recchi[1], Pierre Morsomme[2], Jaak Jaeken[3], Gert Matthijs[4], Geoffroy De Bettignies[1] and François Foulquier[1,*]

[1]Univ. Lille, CNRS, UMR 8576 – UGSF – Unité de Glycobiologie Structurale et Fonctionnelle, F-59000 Lille, France, [2]Institut des Sciences de la Vie, Université Catholique de Louvain, B-1348, Louvain-la-Neuve, Belgium, [3]Center for Metabolic Diseases, University Hospital Gasthuisberg, KU Leuven, Belgium and [4]Center for Human Genetics, KU Leuven, Leuven, Belgium

*To whom correspondence should be addressed at: Univ. Lille, CNRS, UMR 8576 – UGSF – Unité de Glycobiologie Structurale et Fonctionnelle, F-59000 Lille, France. Tel: +33 3 20 43 44 30; Fax: +33 3 20 43 65 55; Email: francois.foulquier@univ-lille1.fr

Abstract

Congenital disorders of glycosylation (CDG) are severe inherited diseases in which aberrant protein glycosylation is a hallmark. From this genetically and clinically heterogenous group, a significant subgroup due to Golgi homeostasis defects is emerging. We previously identified TMEM165 as a Golgi protein involved in CDG. Extremely conserved in the eukaryotic reign, the molecular mechanism by which TMEM165 deficiencies lead to Golgi glycosylation abnormalities is enigmatic. As *GDT1* is the ortholog of *TMEM165* in yeast, both *gdt1*Δ null mutant yeasts and *TMEM165* depleted cells were used. We highlighted that the observed Golgi glycosylation defects due to Gdt1p/TMEM165 deficiency result from Golgi manganese homeostasis defect. We discovered that in both yeasts and mammalian Gdt1p/TMEM165-deficient cells, Mn^{2+} supplementation could restore a normal glycosylation. We also showed that the GPP130 Mn^{2+} sensitivity was altered in *TMEM165* depleted cells. This study not only provides novel insights into the molecular causes of glycosylation defects observed in TMEM165-deficient cells but also suggest that TMEM165 is a key determinant for the regulation of Golgi Mn^{2+} homeostasis.

Introduction

Congenital disorders of glycosylation (CDG) are a rapidly growing disease family due to genetic defects of protein and lipid glycosylation (1–4). In protein N-glycosylation, two different CDG groups can be distinguished. In CDG-I, the molecular defects affect the oligosaccharidic precursor assembly pathway in the endoplasmic reticulum, leading to the presence of unoccupied N-glycosylation sites. CDG-II are due to defects in the glycan processing in the Golgi, giving rise to the presence of abnormal glycan structures on glycoproteins (5,6). To date, the CDG family comprises nearly hundred disorders (7). Most are due to defects in the specific glycosylation machinery, such as SLC35A1 [MIM 605634], B4GALT1 [MIM 137060] and MGAT2 [MIM 602616]) (8–10). However, in the CDG-II group, defects have lately been discovered in proteins that are not only involved in glycosylation but also in other cellular functions. Among these are CDG caused by altered

Received: December 9, 2015. **Revised and Accepted:** January 26, 2016

vesicular Golgi trafficking and/or Golgi pH homeostasis marking a new era in the CDG field (11–16).

In 2012, we reported a novel disorder in this group namely TMEM165-CDG (17) (OMIM entry #614727). These patients present a peculiar phenotype including major skeletal dysplasia and hyposialylation and hypogalactosylation of N-glycosylproteins (17,18). TMEM165 is a transmembrane protein of 324 amino acids belonging to a well conserved but uncharacterized family of membrane proteins named UPF0016 (Uncharacterized Protein Family 0016; Pfam PF01169). We demonstrated that TMEM165 is a novel Golgi protein that can also be found in endocytic pathways (late endosomes and lysosomes) (19). We indirectly demonstrated that defects in TMEM165 affect both cytosolic Ca^{2+} and lysosomal pH homeostasis (20). Based on these results, we then hypothesized that TMEM165 could be a Golgi-localized Ca^{2+}/H+ antiporter regulating both Golgi Ca^{2+} and pH homeostasis (20). Extremely conserved in the eukaryotic reign, *GDT1* is the yeast ortholog of *TMEM165*. We showed that the gdt1Δ mutant presents a strong growth defect phenotype in presence of high concentrations of calcium chloride (500–700 mM). In yeast, the Ca^{2+} Golgi homeostasis mainly results from the activity of Pmr1p, a Golgi P-type ATPase essential to import Ca^{2+} but also Mn^{2+} in the Golgi lumen (21–23). Its activity then maintains very low Ca^{2+} and Mn^{2+} concentrations into the cytosol. Interestingly, it has been shown that *Pmr1* inactivation leads to strong Golgi glycosylation and trafficking defects (24).

The aim of this study is to decipher the molecular mechanism by which a lack of TMEM165 affects Golgi glycosylation. We used *gdt1* null mutant yeasts and TMEM165 depleted mammalian cells to unravel this mechanism, and present evidence that in both yeasts and mammalian cells, the Golgi glycosylation defects due to a lack of Gdt1p/TMEM165, result from defective Golgi manganese homeostasis.

Results

Mn^{2+} suppresses the Golgi glycosylation defect of *gdt1Δ* null mutants cultured in presence of high Ca^{2+} concentrations

We previously reported that *gdt1Δ* null mutants presented a strong growth defect in the presence of high calcium chloride concentrations such as 700 mM (25). To assess whether this growth deficiency was correlated to an abnormal N-linked glycosylation, the gel mobility of secreted invertase, a protein exclusively N-glycosylated and thus a good reporter of Golgi N-glycosylation efficiency *in vivo* was analyzed in the absence and in the presence of increasing Ca^{2+} concentrations (Fig. 1A). In yeast, pmr1p is a Golgi Ca^{2+}/Mn^{2+} P-type ATPase that is involved in maintaining normal Golgi functions, such as glycosylation (21–23). Thus, *Pmr1Δ* strains, known to produce and secrete an aberrant form of invertase, lacking high mannose residues, were taken as positive controls throughout our experiments (21,23).

While invertase isolated from *pmr1Δ* strain migrates on native gels significantly faster than invertase isolated from a wild-type strain, no significant differences in the absence of Ca^{2+} were observed between *gdt1Δ* and wild-type strains. Strikingly and in the

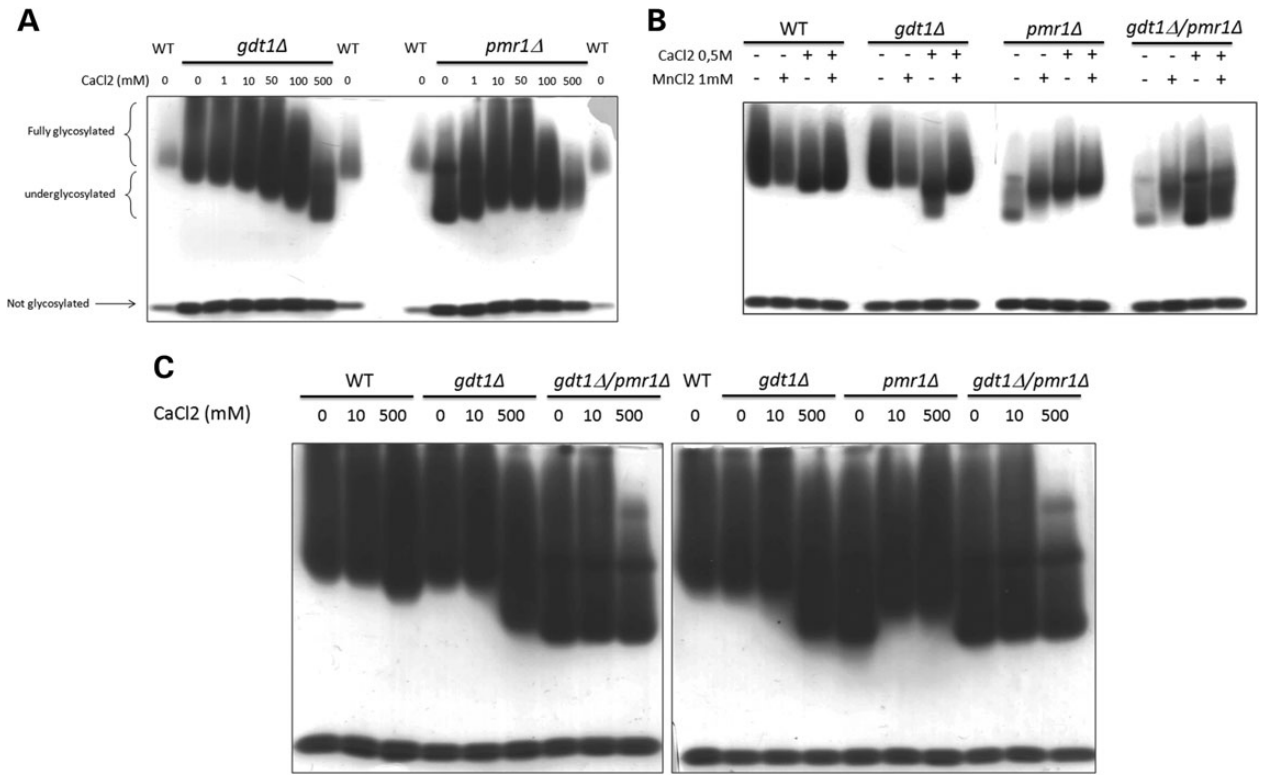

Figure 1. Mn^{2+} restores the Golgi glycosylation defect of *gdt1Δ* null mutants cultured in the presence of high Ca^{2+} concentrations. (**A**) High Ca^{2+} concentrations strongly affect invertase glycosylation in *gdt1Δ* strains and partially suppress the glycosylation defect in *pmr1Δ* strains. N-Glycosylated invertase secreted by wild type, *gdt1Δ* and *pmr1Δ* mutants with or without the addition of the indicated $CaCl_2$ concentrations in the medium. (**B**) Mn^{2+} suppresses the glycosylation defect of the *gdt1Δ* strains cultured with 0.5 M $CaCl_2$. N-Glycosylated invertase secreted by wild type, *gdt1Δ* strains, *pmr1Δ* and *gdt1Δ/pmr1Δ* strains with or without the addition of 0.5 M $CaCl_2$, with or without the addition of Mn^{2+}, or with the addition of both 0.5 M $CaCl_2$ and 1 mM $MnCl_2$. (**C**) gdt1p is involved in the suppression of the glycosylation defect in the *pmr1Δ* strains cultured in high Ca^{2+} concentration. N-Glycosylated invertase secreted by wild-type, *gdt1Δ* strains, *pmr1Δ* and *gdt1Δ/pmr1Δ* strains with or without the addition of 0.5 M $CaCl_2$ or 10 mM $CaCl_2$.

presence of increasing Ca^{2+} concentrations, invertase secreted from *gdt1Δ* strain migrates faster. In wild-type strains, increasing Ca^{2+} concentrations had no effects on invertase mobility (data not shown). As seen in other studies, the increased mobility observed in pmr1p mutant cells cultured in the absence of Ca^{2+} can partially be reversed in the presence of Ca^{2+} (22). These data demonstrate that high environmental Ca^{2+} concentrations in *gdt1Δ* lead to strong N-glycosylation deficiencies while in *pmr1Δ*, the observed Golgi N-glycosylation defects are markedly restored by Ca^{2+}.

In order to understand how high Ca^{2+} concentrations in *gdt1Δ* could lead to glycosylation abnormalities, we hypothesized that excess of Ca^{2+} might interfere with glycosylation processes requiring other metal ions including Mn^{2+} known to be a cofactor of certain Golgi glycosyltransferases (26). To test this hypothesis, the invertase mobility was assessed by supplementing the culture medium with 1 mM $MnCl_2$ (Fig. 1B). While this treatment does not affect the invertase mobility in wild-type strain, Mn^{2+} treatment completely restores the increased invertase mobility in *gdt1Δ* strains cultured in the presence of both Ca^{2+} and Mn^{2+}. As previously reported, the Mn^{2+} supplementation in *pmr1Δ* mutant also greatly improves the invertase mobility (22). This complementation is highly specific for Mn^{2+} as other tested ions do not rescue the glycosylation phenotype (Supplementary Material, Fig. S1). In order to understand the link between gdt1p and pmr1p, invertase mobility was analyzed in the *gdt1Δ/pmr1Δ* double knockout. In normal conditions, the invertase mobility is strongly affected and very similar to the one observed in the *pmr1Δ* strains. While Mn^{2+} slightly suppressed this Golgi N-glycosylation defect, Ca^{2+} did not. Very interestingly, this result seems to show that gdt1p is then crucial for the suppression of the glycosylation defect in the *pmr1Δ* strains supplemented with Ca^{2+}. However, since 0.5 M $CaCl_2$ already leads to a strong invertase mobility defect in *gdt1Δ* strains, a 10 mM $CaCl_2$ concentration was used. In these conditions, no glycosylation defect was observed in *gdt1Δ* strains, while in *pmr1Δ* strains 10 mM $CaCl_2$ was sufficient to suppress the glycosylation defect (Fig. 1A and C). However, this low concentration was not sufficient to rescue the invertase mobility in the *gdt1Δ/pmr1Δ* double knock-out, demonstrating a crucial need for gdt1p in this rescue (Fig. 1C).

These unexpected findings not only demonstrate that the observed Golgi N-glycosylation defect in *gdt1Δ* strains cultured in the presence of high Ca^{2+} concentrations can be suppressed by the addition of Mn^{2+} but also that gdt1p is directly involved in the suppression of the glycosylation defect in the *pmr1Δ* strains supplemented with Ca^{2+}. Altogether, one can ask the role of gdt1p in Golgi Mn^{2+} homeostasis.

Golgi manganese homeostasis is modified in TMEM165-deficient cell lines

In order to unravel the link between TMEM165, Golgi Mn^{2+} homeostasis and Golgi glycosylation defects, TMEM165 expression was depleted using shRNA strategy in HeLa and HEK 293 cells. In order to avoid the issue of clonal variation, polyclonal populations of stably expressing cells were generated and used for the study. ShRNA depletion of TMEM165 in HeLa and HEK 293 cells was very efficient as 95% of TMEM165 was depleted compared with control cells (Fig. 2A and C). This decrease was also confirmed by immunofluorescence staining. As shown in Figure 2B and D, TMEM165 is absent in TMEM165-depleted cells.

To then assess the Mn^{2+} Golgi homeostasis in TMEM165-depleted cells, we took advantage of the Golgi protein GPP130 that is known to be a specific Golgi Mn^{2+} sensor (27,28). In mammalian cell lines, it has been shown by several authors that the stability of GPP130 was strictly dependent on Golgi Mn^{2+} concentration. In the presence of 500 μM $MnCl_2$, GPP130 was shown to be targeted to lysosomal degradation via a Rab7-dependent mechanism (28). The stability of GPP130 was studied with and without $MnCl_2$ treatment by western blot and immunofluorescence in shTMEM165 HeLa and HEK293 cells (Figs 3 and 4). In accordance with the literature, we showed that the level of GPP130 was significantly reduced when control cells were cultured with Mn^{2+} (Figs 3A and 4A and quantification in Figs 3B and 4B). Interestingly, this Mn^{2+}-induced degradation is strongly delayed in TMEM165-depleted cells. Quantification indicated that GPP130 loss exceeded 60% in control HeLa cells after 4 h Mn^{2+} treatment while only a 20% decrease is seen in shTMEM165 HeLa cells. We can notice that in HEK293 cells, the effects of Mn^{2+} on GPP130 stability are less pronounced as GPP130 loss exceeded only 40% in control HEK293 cells after 16 h of Mn^{2+} treatment. Similarly to shTMEM165 HeLa cells, the Mn^{2+} treatment had no effects on GPP130 stability in shTMEM165 HEK293 cells. Immunofluorescence staining followed by confocal microscopy confirmed the western blot results for both HeLa and HEK293 cells (Figs 3C and 4C and quantification in Figs 3D and 4D). Altogether, these data highly suggest that the Golgi Mn^{2+} homeostasis is impaired in TMEM165-depleted cells.

As shown by Mukhopadhyay and collaborators, high concentrations of extracellular Mn^{2+} induces rapid redistribution of GPP130 in vesicles before their lysosomal degradation. As HeLa cells were shown to be more sensitive to Mn^{2+} treatment, we decided to investigate the differential impact of Mn^{2+} on the vesicular redistribution of GPP130 in shTMEM165 HeLa cells compared with control cells. The redistribution of GPP130 was followed by immunofluorescence in response to different times of Mn^{2+} exposure (Fig. 5). In the absence of Mn^{2+}, GPP130 is Golgi localized in both control and shTMEM165 HeLa cells (Fig. 5A and C). After 1 and 2 h of Mn^{2+} treatment in control cells, GPP130 is delocalized in punctate structures (~20 GPP130 positive structures per cell have been quantified) decreasing to <10 positive structures per cell after 4 h of Mn^{2+} treatment. Remarkably and after Mn^{2+} exposure, the number of positive GPP130 punctuate structures in shTMEM165 cells is extremely low (~5 per cell). This confirms the western blot result and demonstrates the insensitivity of GPP130 to Mn^{2+} treatment in shTMEM165 HeLa cells. As the GPP130 luminal stem domain has been demonstrated to confer this Mn^{2+} sensitivity, our results highly suggest that TMEM165 is required to regulate Golgi Mn^{2+} homeostasis.

TMEM165 knockdown provokes a glycosylation defect that can be suppressed by manganese supplementation

As we previously showed that Golgi glycosylation deficiency in *gdt1Δ* strains can be suppressed by the addition of $MnCl_2$ in the medium, we wanted to investigate in TMEM165-depleted cells (i) the glycosylation defect and (ii) the impact of Mn^{2+} supplementation on the suppression of the glycosylation defect. To evaluate these two aspects, we first determined the steady-state glycosylation status of LAMP2, an extensively N-glycosylated lysosomal resident protein and TGN46, a glycoprotein known to be N- and O-glycosylated. For this, control and shTMEM165 HeLa and HEK293 cells were treated or not with $MnCl_2$ (Fig. 6). While a subtle change in the LAMP2 mobility arguing for slight heterogeneity in glycosylation could be observed between control and shTMEM165 HeLa cells (Fig. 6A), a more pronounced decrease in TGN46 molecular weight was observed compared with control cells (Fig. 6A). Remarkably, when Mn^{2+} was added to the cell culture, the altered gel mobility of LAMP2 and TGN46 was completely suppressed in shTMEM165

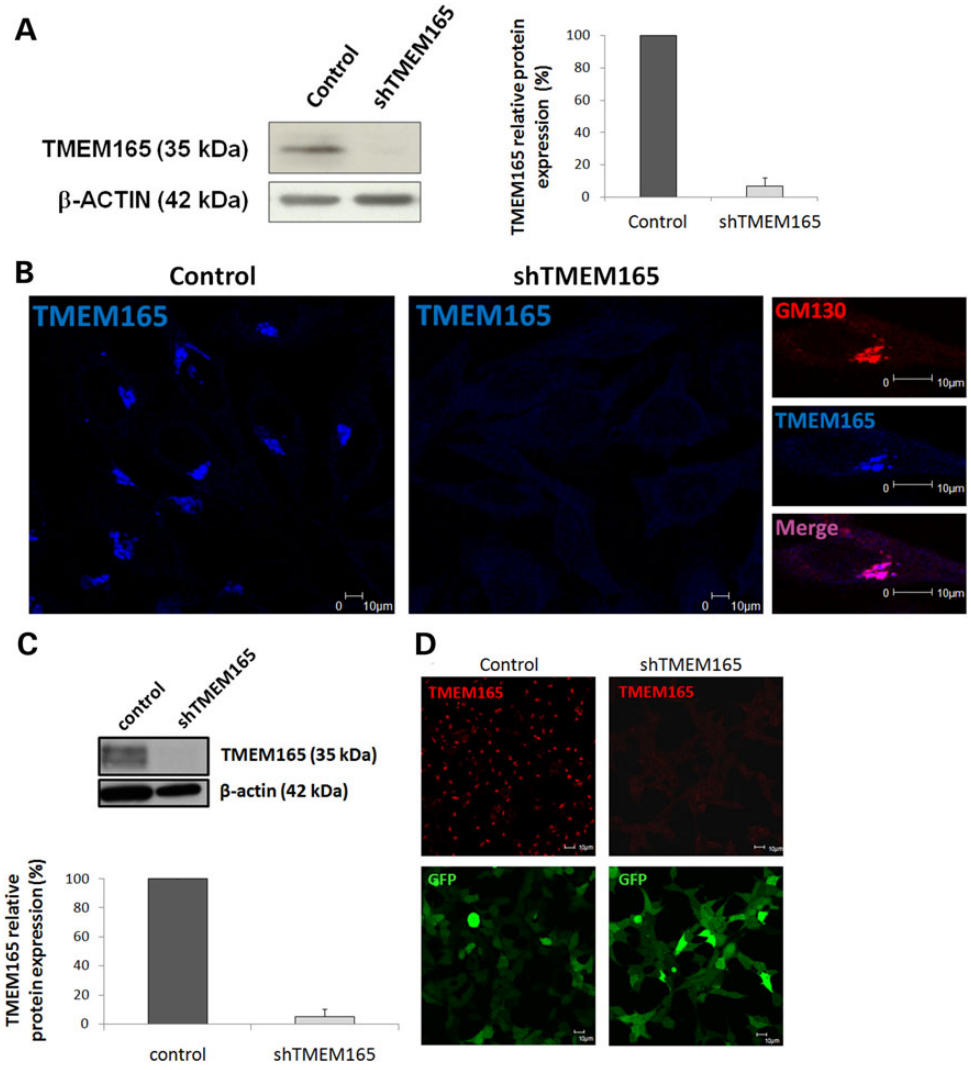

Figure 2. Generation and characterization of shTMEM165 HeLa and HEK293 cells. (**A**) Steady-state cellular level of TMEM165. HeLa cells were mock (control) or depleted in TMEM165 (shTMEM165). Total cell lysates were prepared, subjected to SDS–PAGE and western blot with the indicated antibodies. Right panel represents quantification of TMEM165. (**B**) Control and shTMEM165 HeLa cells were fixed and labeled with antibodies against TMEM165 and GM130 before confocal microscopy visualization. (**C**) Steady-state cellular level of TMEM165. HEK293 cells were mock (control) or depleted in TMEM165 (shTMEM165). Total cell lysates were prepared, subjected to SDS–PAGE and western blot with the indicated antibodies. Lower panel represents quantification of TMEM165. (**D**) Control and shTMEM165 HEK293 cells were fixed and labeled with antibodies against TMEM165 before confocal microscopy visualization. Lower panel shows the GFP, coded by the pGIPZ Lentiviral shRNA plasmid (Thermo Scientific) used for the generation of our cell lines.

HeLa cells. Comparable with the shTMEM165 HeLa results, a stronger increase in both LAMP2 and TGN46 gel mobility was observed in shTMEM165 HEK293 cells (Fig. 6B). Very interestingly, the observed increased gel mobility was also suppressed for these two glycoproteins after Mn^{2+} treatment. To appreciate the specific effect of the Mn^{2+}, shTMEM165 HEK293 cells were treated with $MnSO_4$. Similarly to $MnCl_2$, $MnSO_4$ completely suppresses the observed heterogeneity in gel mobility (Supplementary Material, Fig. S2). To confirm that Mn^{2+} rescues the glycosylation process, shTMEM165 HEK293 cells treated or not with Mn^{2+}, were subjected to PNGase F treatment (Supplementary Material, Fig. S3). We found that deglycosylation of LAMP2 produced a 40 kDa polypeptide for both (Supplementary Material, Fig. S3A). For TGN46 and in the absence of Mn^{2+}, PNGase F treatment leads only to a slight increase in gel mobility arguing that among the potential N-glycosylation sites of TGN46, only few of them are N-glycosylated (Supplementary Material, Fig. S3B). We interestingly found that deglycosylation of TGN46 from shTMEM165 HEK293 cells treated with Mn^{2+} produces a band with a higher molecular weight than the one obtained in untreated shTMEM165 cells. Altogether, these results suggest that Mn^{2+} rescues the N-glycosylation for LAMP2 and likely the O-glycosylation for TGN46. It is important to note that the glycosylation defect observed for both LAMP2 and TGN46 in shTMEM165 HEK293 cells does not lead to an aberrant subcellular localization for these two proteins (Supplementary Material, Fig. S4).

To confirm the Mn^{2+} effects, mass spectrometry analysis of N-glycans was performed in control and shTMEM165 HEK293 cells treated or not with Mn^{2+} (Fig. 7). The structures detected at mass-per-charge (m/z) ratios >2966 were found absent in shTMEM165 HEK293 cells compared with control cells then demonstrating a severe Golgi processing defect. Remarkably, the structures detected at mass-per-charge (m/z) ratios 1345, 1416, 1591, 1836, 1907, 2040, 2081, 2285, 2326, 2850 and 2891 were found in increased abundance in shTMEM165 cells in comparison with those

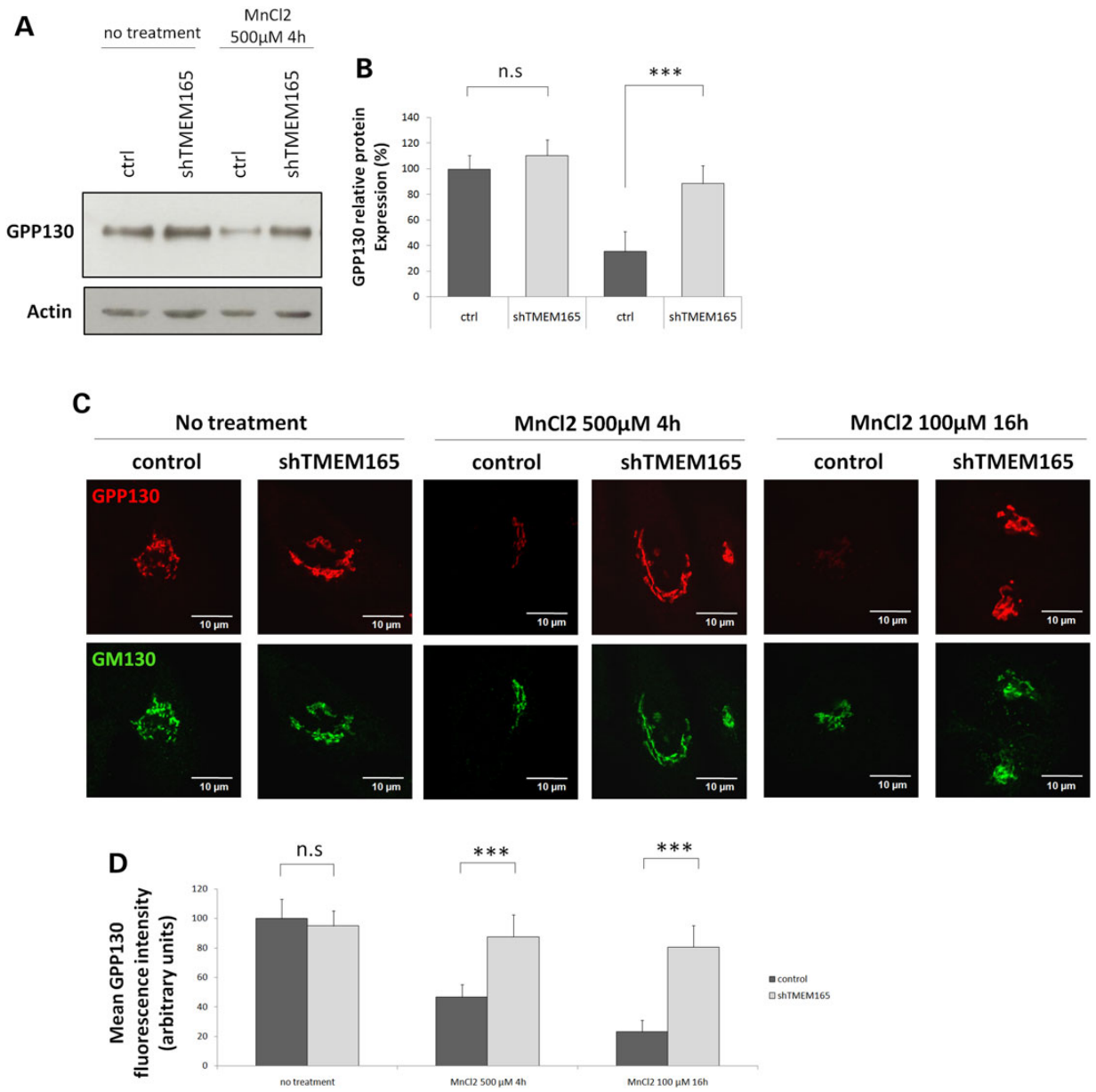

Figure 3. Mn^{2+} does not alter the stability of GPP130 in TMEM165-deficient HeLa cell lines (**A**) Steady-state cellular level of GPP130. Control and shTMEM165 HeLa cells were treated or not with $MnCl_2$ 500 µM during 4 h. Total cell lysates were prepared, subjected to SDS–PAGE and western blot with the indicated antibodies. (**B**) Quantification of GPP130 protein after normalization with actin ($N = 3$; ***P-value <0,001). (**C**) Control and shTMEM165 HeLa cells were incubated with $MnCl_2$ 500 µM during 4 h or 100 µM during 16 h, fixed and labeled with antibodies against GPP130 (upper panels) and GM130 (lower panels) before confocal microscopy visualization. (**D**) Quantification of the associated GPP130 fluorescence intensity (number of experiments (N) = 3; number of cells (n) = 50; ***P-value <0.001).

observed in control cells. These results highlight a strong galactosylation, a moderate GlcNAcylation defect and a very slight sialylation defect in shTMEM165 HEK293 cells. While Mn^{2+} treatment have no obvious effects on control HEK293 cells, such treatment largely suppresses the observed glycosylation defects, mainly the galactosylation defect, as observed by the decreased abundance of the structures (m/z) 1836 and 2081. This demonstrates that a defect in TMEM165 impairs the function of Golgi Mn^{2+}-dependent enzymes, mainly the β-1,4-galactosyltransferase I. As Mn^{2+} supplementation could be considered as a treatment option, different Mn^{2+} concentrations (1–50 µM) have been tested. Interestingly, we observe that only 1 µM was sufficient to completely suppress the glycosylation defect observed in shTMEM165 HEK293 cells for both TGN46 and LAMP2 (Fig. 8). Altogether and in agreement with the yeast results, we demonstrated that (i) the underlying pathomechanism of TMEM165 deficiency is linked to Golgi Mn^{2+} homeostasis defect and (ii) the impaired Golgi glycosylation could totally be rescued by the addition of Mn^{2+}.

Discussion

TMEM165 deficiency was recently found to lead to a type-II CDG associated with defective Golgi N-glycosylation. TMEM165/Gdt1p is extremely conserved during evolution, and has no known direct molecular function. TMEM165/Gdt1p is not directly involved in the Golgi glycosylation process, as it is neither a sugar transporter nor

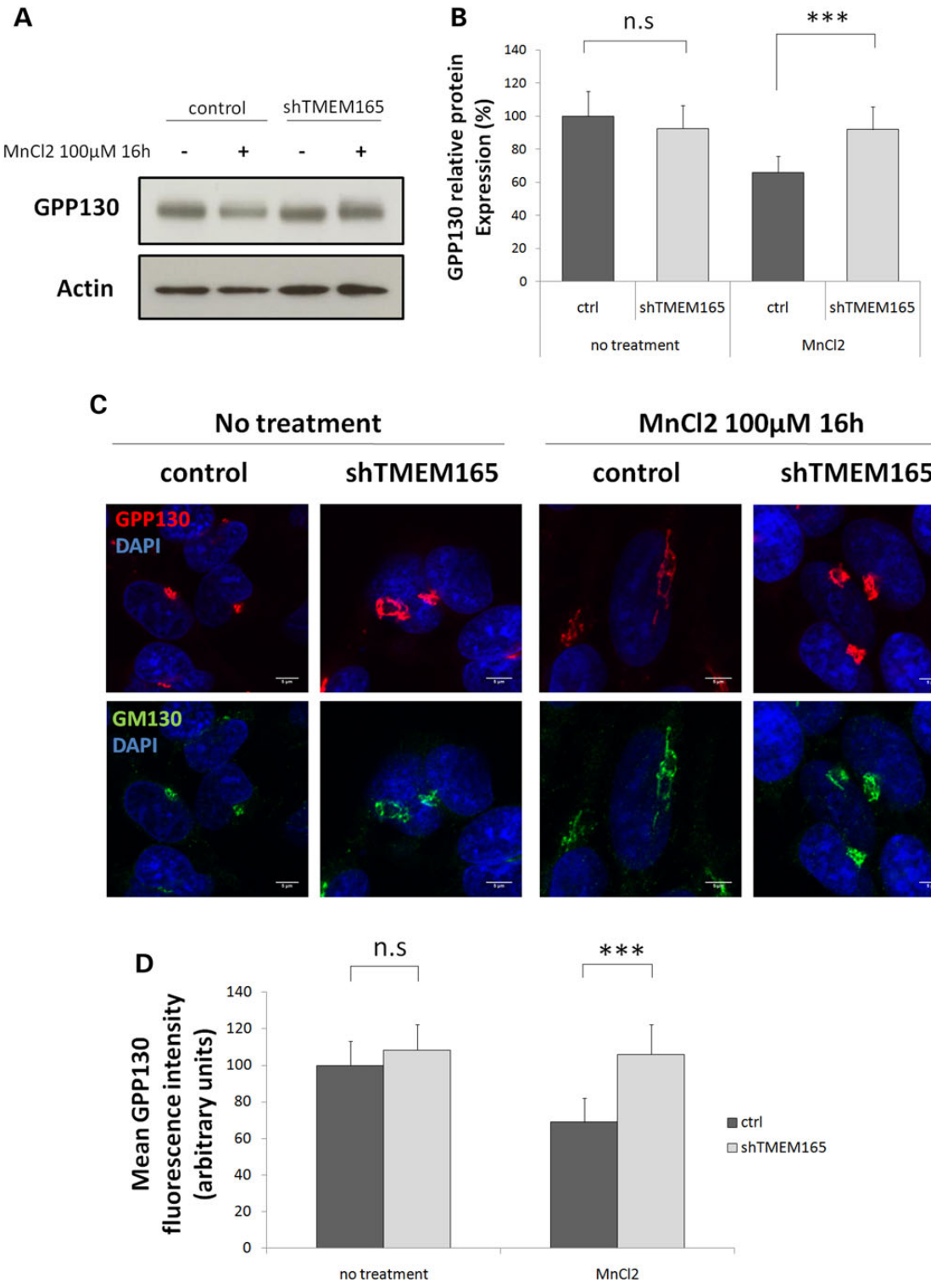

Figure 4. Mn^{2+} does not alter the stability of GPP130 in TMEM165-deficient HEK293 cell lines. (**A**) Steady-state cellular level of GPP130. Control and shTMEM165 HEK293 cells were treated or not with $MnCl_2$ 100 µM during 16 h. Total cell lysates were prepared, subjected to SDS–PAGE and western blot with the indicated antibodies. (**B**) Quantification of GPP130 protein after normalization with actin (N = 2; ***P-value <0.001). (**C**) Control and shTMEM165 HEK293 cells were incubated with $MnCl_2$ 100 µM during 16 h, fixed and labeled with antibodies against GPP130 (upper panels) and GM130 (lower panels) before confocal microscopy visualization. DAPI staining was performed and shows the nucleus. (**D**) Quantification of the associated GPP130 fluorescence intensity (number of experiments (*N*) = 2; number of cells (*n*) = 50; ***P-value <0.001).

a Golgi glycosyltransferase. Previous work has shown that a lack of Gdt1p leads to a sensitivity to high Ca^{2+} concentrations and we have demonstrated that TMEM165 is involved in pH homeostasis (20). These results led us to hypothesize that Gdt1p/TMEM165 could be a Ca^{+}/H^{+} antiporter involved in the Golgi Ca^{2+} entrance and exit of H+. In this study, we showed that high environmental

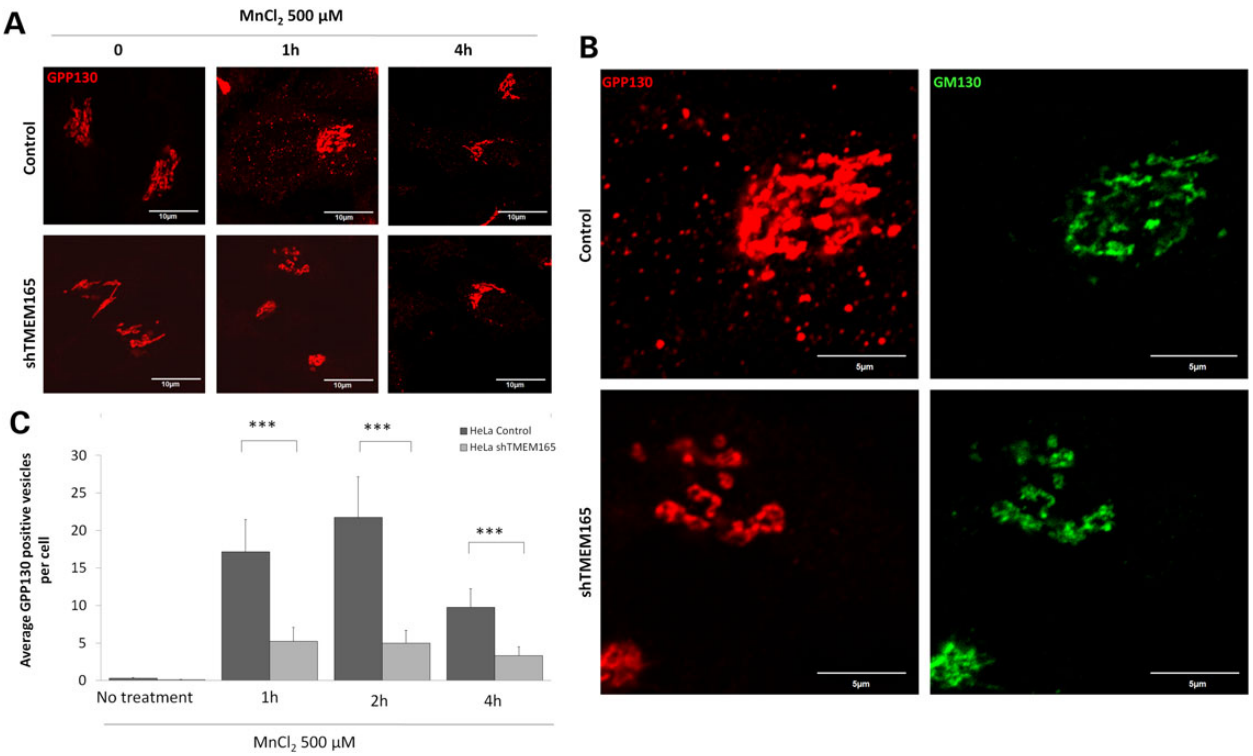

Figure 5. Alteration of the Mn^{2+} associated GPP130 vesicularization in shTMEM165 cells. (**A**) Control and shTMEM165 HeLa cells were incubated with $MnCl_2$ 500 µM during the indicated times, fixed and labeled with antibodies against GPP130 (upper panels) and GM130 (lower panels) before confocal microscopy visualization. (**B**) Magnification of the 1 h panel presented in A. Cells were immunostained with anti-GPP130 (left panels) and anti-GM130 antibodies (right panels). (**C**) Quantification of the average number of GPP130 positive vesicles per cell in control and shTMEM165 HeLa cells ($N = 2$; $n = 50$; ***P-value <0.001).

Ca^{2+} concentrations in *gdt1Δ* led to strong N-glycosylation deficiencies while in *pmr1Δ*, the observed Golgi N-glycosylation defects were markedly suppressed in the presence of Ca^{2+}. This antagonistic effect then implied different functions for these two proteins. Interestingly, previous work has also shown that the observed Golgi glycosylation defects in *pmr1Δ* were not due to the lack of Ca^{2+} uptake but mainly to a lack of Mn^{2+} uptake. Moreover, adding Mn^{2+} to the culture medium can rescue the N-glycosylation defect of the *pmr1Δ* strains (22). We therefore hypothesized that the observed glycosylation defect in *gdt1Δ* could also be linked to a decrease in Mn^{2+} Golgi homeostasis. In that case, the addition of Mn^{2+} to the culture medium could be sufficient to complement the glycosylation deficiency observed in the presence of high Ca^{2+} concentrations. In order to explore this hypothesis, Mn^{2+} and other cations were tested in *gdt1Δ* yeasts. Interestingly, 1 mM $MnCl_2$ was sufficient to completely suppress the glycosylation deficiency seen in the presence of high calcium concentration.

Why is the glycosylation deficiency only seen in the presence of high calcium concentration in *gdt1Δ* yeasts? One part of the answer certainly resides in the fact that Pmr1p is a Ca^{2+}/Mn^{2+} transporter. It is then tempting to hypothesize that a high Ca^{2+} concentration could prevent the import of Mn^{2+} via Pmr1p into the Golgi via a dilution phenomenon. In the absence of Gdt1p, the import of Mn^{2+} into the Golgi compartment would not be sufficient to generate the Mn^{2+} homeostasis required for Golgi glycosyltransferases activities. The Mn^{2+}-dependent catalytic activity is indeed a characteristic of many Golgi glycosyltransferases in yeasts such as MNN1, MNN2 and MNN5 (29,30). Therefore and in the presence of high Ca^{2+} concentration, their activities would be likely altered in the absence of Gdt1p.

The other possibility that we cannot completely exclude is a direct competition between Ca^{2+} and Mn^{2+} inside the Golgi lumen. In that case, Gdt1p would function as an extruder of Ca^{2+} from the Golgi lumen to lower the competition between Ca^{2+} and Mn^{2+}. The Mn^{2+} import into the Golgi could also be indirect. Two Mn^{2+} transporters exist in the yeast secretory pathway, Smf1p and Smf2p that allows the Mn^{2+} import in the ER and TGN/endosomes, respectively. One can then imagine that the lack of Gdt1p disturbs the functions and/or localization of these transporters in the presence of high Ca^{2+} concentration then causing indirectly a deficiency of Golgi Mn^{2+} import (31). Interestingly, we also showed that gdt1p is directly involved in the suppression of the glycosylation defect in the *pmr1Δ* strains supplemented with Ca^{2+}. This suggests that the presence of Ca^{2+} increases the Golgi Mn^{2+} uptake, and that this molecular process is mediated by gdt1p. From these yeast data, we could propose a model where Gdt1p would act as an antiporter or cotransporter of Mn^{2+}/Ca^{2+}. As an abnormal lysosomal pH has been highlighted in TMEM165-deficient CDG patients, we could imagine that the used counterion for Mn^{2+} entry would be different, H+ for mammalian cells and Ca^{2+} for yeasts.

As the regulation of Mn^{2+} homeostasis is highly conserved between yeasts and higher eukaryotes, we assessed the impact of Mn^{2+} on Golgi glycosylation in TMEM165-depleted cells (HeLa and HEK293). We first wanted to highlight that the Golgi Mn^{2+} homeostasis was impaired in TMEM165-depleted cells by using GPP130 as an intra-Golgi Mn^{2+} sensor. We clearly showed that in TMEM165-depleted cells, compared with control cells, the GPP130 Mn^{2+} sensitivity was altered. As the luminal stem domain was sufficient to confer Mn^{2+} sensitivity to the protein, our results support a model where the Golgi Mn^{2+} homeostasis would be disrupted in TMEM165-depleted cells. Interestingly, we observed that the effect of shTMEM165 on GPP130 degradation was stronger in HeLa when compared with HEK293 cells. The Mn^{2+} concentration inside the Golgi is mainly depending of two

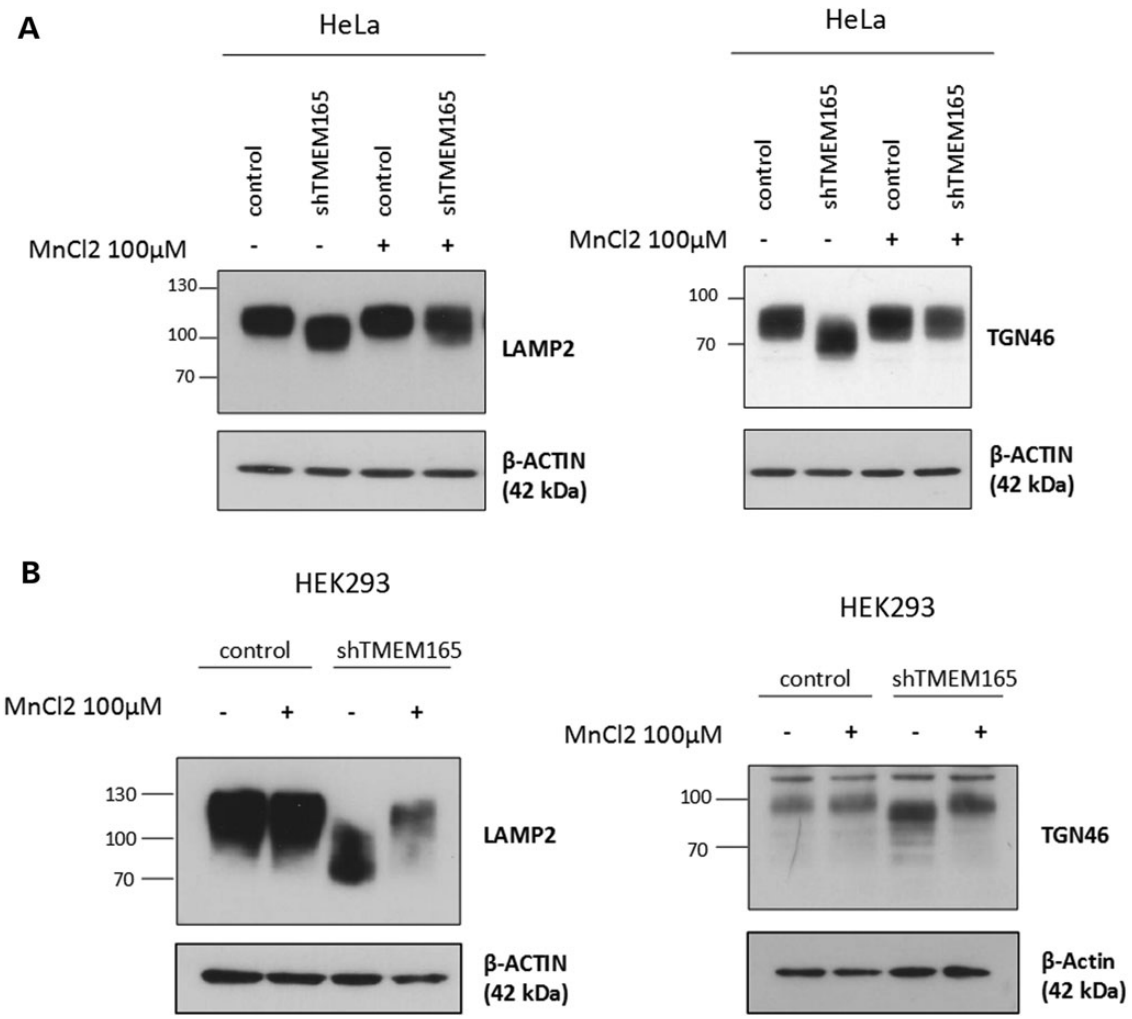

Figure 6. Mn^{2+} suppresses the observed LAMP2 and TGN46 altered gel mobility in TMEM165-depleted cells. (**A**) Steady-state cellular level and gel mobility of LAMP2 and TGN46 in control and shTMEM165 HeLa cells. (**B**) Steady-state cellular level and gel mobility of LAMP2 and TGN46 in control and shTMEM165 HEK293 cells. Control and shTMEM165 cells were cultured in the absence or presence of $MnCl_2$ (100 µM) during 18 h, cell lysates were prepared, subjected to SDS–PAGE and western blot with the indicated antibodies.

factors (i) the uptake of Mn^{2+} from the cytosol into the Golgi (mainly depending of the Ca^{2+}/Mn^{2+}-ATPase and certainly other transporters) and (ii) the intake of Mn^{2+} from the extracellular medium into the cytosol (depending of the plasma membrane expression of Mn^{2+} transporters). As increased Mn^{2+} concentration in the culture medium has a stronger effect on GPP130 degradation in HeLa cells as compared to HEK293 cells, one can suppose that the Mn^{2+} intake is very efficient in HeLa compared to HEK293 cells. This could also explain why the glycosylation defect is very subtle in HeLa cells compared with HEK293 cells.

The impact of Mn^{2+} on Golgi glycosylation was assessed by mass spectrometry and by following the migration profile of two highly glycosylated proteins. While the migration was shown to be altered for both LAMP2 and TGN46 in both shTMEM165 HeLa and HEK293 cells, the Mn^{2+} treatment did completely restore a protein mobility comparable with that observed in control cells Analysis of N-linked glycans from glycoproteins using MALDI-TOF mainly showed the accumulation of agalactosylated glycan structures in TMEM165-depleted HEK293 cells arguing for a severe galactosylation defect. In line with the western blot results, Mn^{2+} treatment almost totally suppressed the observed glycosylation defect. This galactosylation defect is very interesting and seems to be a general characteristic of the cellular Mn^{2+} impairment. The recent discovery of CDG patients presenting strong galactosylation defects on serotransferrin and carrying SLC39A8 mutations, a Zn^{2+}/Mn^{2+} transporter, emphasizes the link between Golgi Mn^{2+} homeostasis and Golgi galactosylation efficiency process (32). Two Golgi galactosyltransferases are known to transfer Gal residues from UDP-Gal to terminal *N*-acetylglucosamine (GlcNAc) residues, the UDP-Gal:*N*-acetylglucosamine β-1,4-galactosyltransferase I (B4GALT1; EC 2.4.1.22) that synthesizes *N*-acetyl lactosamine structures on glycoproteins and the UDP-Gal:*N*-acetylglucosamine β-1,4-galactosyltransferase II (B4GALT2; EC 2.4.1.22) that both act on glycoproteins and glycolipids. From a general point of view, these enzymes as well as the Golgi glycosyltransferases using UDP-sugars as a donor substrate, absolutely require Mn^{2+} for their activities. This could also explain why the GlcNAcylation process is also impaired in TMEM165-depleted HEK293 cells.

Altogether, these experiments confirmed that in both yeasts and mammalian cells, the glycosylation abnormalities due to Gdt1p/TMEM165 defects are rescued by the addition of Mn^{2+}.

In conclusion, we demonstrated that the observed Golgi glycosylation deficiencies in Gdt1p/TMEM165-deficient cells result from a defective Golgi Mn^{2+} homeostasis. This study provides

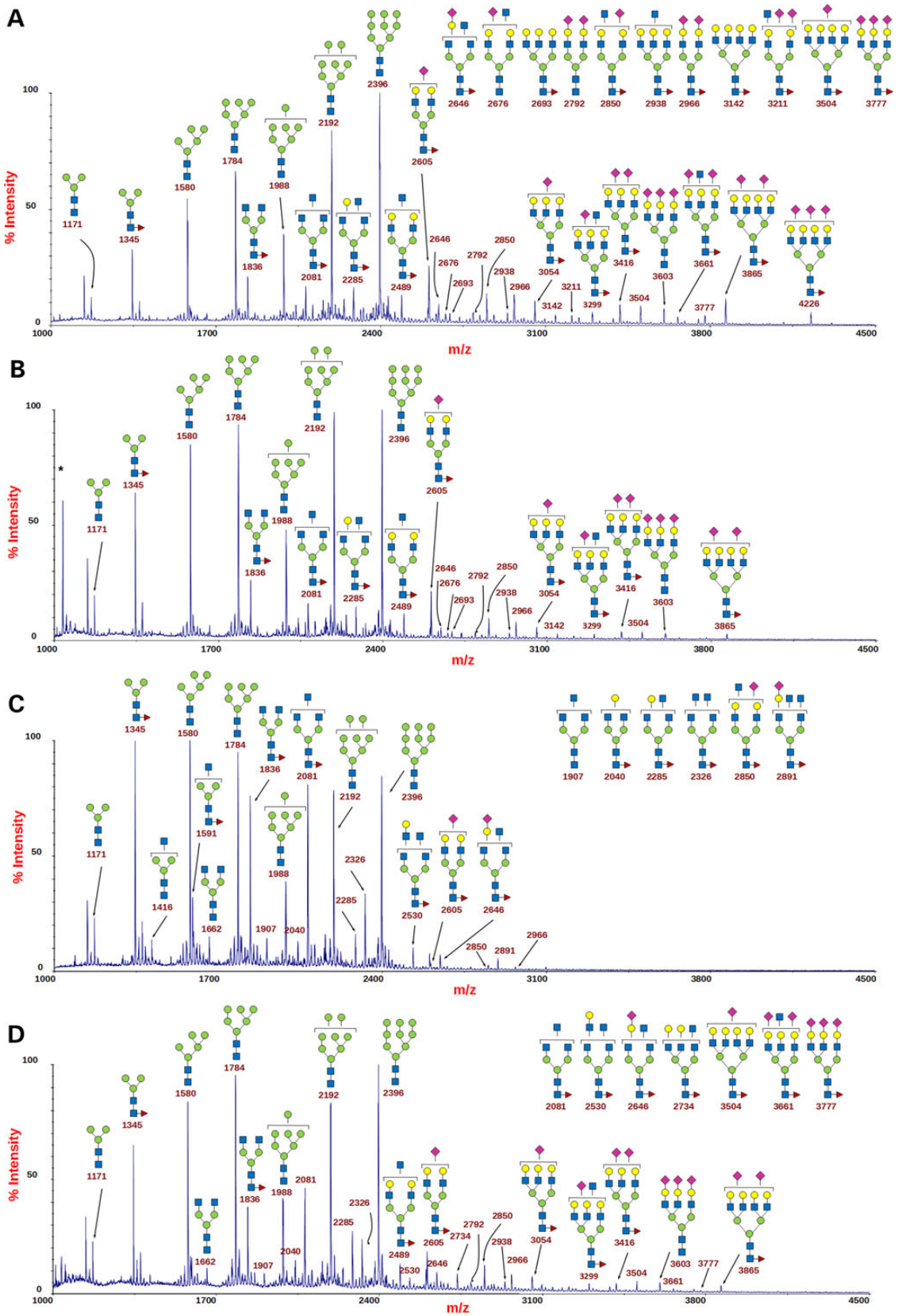

Figure 7. Mn^{2+} suppresses the observed galactosylation defect in TMEM165 depleted cells. (**A**) MALDI-TOF-MS spectra of the permethylated *N*-glycans from control HEK293 cells. (**B**) MALDI-TOF-MS spectra of the permethylated *N*-glycans from control HEK293 cells treated with Mn^{2+} 100 μM for 36 h. (**C**) MALDI-TOF-MS spectra of the permethylated *N*-glycans from shTMEM165 HEK293 cells. (**D**) MALDI-TOF-MS spectra of the permethylated *N*-glycans from shTMEM165 HEK293 cells treated with Mn^{2+} 100 μM for 36 h. The proposed glycan structures are in accordance with the Golgi biosynthetic pathway. The symbols representing sugar residues are as follows: closed square, *N*-acetylglucosamine; open circle, mannose; closed circle, galactose; open diamond, sialic acid; and closed triangle, fucose. Linkages between sugar residues have been removed for simplicity.

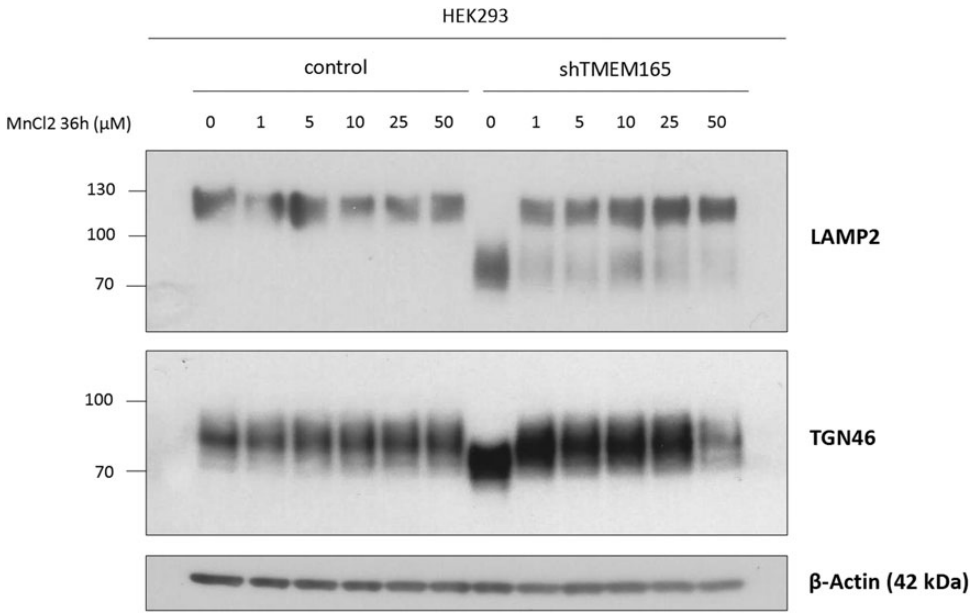

Figure 8. One micromolar of $MnCl_2$ is sufficient to suppress the glycosylation defect observed in shTMEM165 HEK293 cells for both TGN46 and LAMP2. Steady-state cellular level and gel mobility of LAMP2 and TGN46 in control and shTMEM165 HEK293 cells. Cells were cultured in the absence or presence of $MnCl_2$ during 36 h, cell lysates were prepared, subjected to SDS–PAGE and western blot with the indicated antibodies.

novel insights into the mechanism of the galactosylation defect observed in TMEM165-deficient cells. These findings also support the potential use of therapeutic trials of Mn^{2+} in TMEM165-deficient patients.

Material and Methods

Yeast strains and media

Yeast strains originating from BY4741 background used for the experiments are listed

Wild type: Mata his3Δ1 leu2Δ0 ura3Δ0
pmr1Δ: Mata his3Δ1 leu2Δ0 ura3Δ0 pmr1Δ::KanMX4
gdt1Δ: Mata his3Δ1 leu2Δ0 ura3Δ0 gdt1Δ::KanMX4
gdt1Δ /pmr1Δ: Mata his3Δ1 leu2Δ0 ura3Δ0 gdt1Δ::KanMX4 pmr1Δ::KanMX4

Yeasts were cultured at 30°C. Cultures in liquid media are done under a light shaking. Rich media, named YEP media, contains yeast extract (10 g L^{-1}, Difco), Bacto-peptone (20 g L^{-1}, Difco). YPD media is a YEP media supplemented with 2% D-glucose (Sigma-Aldrich). YPR is YEP supplemented with 2% raffinose (Euromedex). Selection antibiotics were added at 100 μg mL^{-1} for nourseothricine and 200 μg mL^{-1} for G418.

Invertase glycosylation analysis

Before any analysis, a preculture in YPD media is done and a volume equivalent to 15 $OD600_{nm}$ units is centrifugated for 3 min at 3500 rpm. The supernatant is discarded and the pellet is resuspended in YPR media to induce invertase expression. Calcium, manganese and other ions were added at this step at the indicated concentration. After a 20 h culture in YPR, yeasts were centrifugated for 5 min at 3500 rpm. Supernatant was discarded and the pellet was kept frozen at –20°C. Invertase glycosylation analysis was performed as described by Ballou *et al.* (33).

Antibodies and other reagents

Anti-TMEM165 and anti-β actin antibodies were from Sigma-Aldrich (St Louis, MO, USA). Anti-GM130 antibody was from BD Biosciences (Franklin lakes, NJ, USA). Anti-GPP130 antibody was purchased from Covance (Princeton, NJ, USA). Goat anti-rabbit or goat anti-mouse immunoglobulins HRP conjugated were purchased from Dako (Glostrup, Denmark). Polyclonal goat anti-rabbit or goat anti-mouse conjugated with Alexa Fluor was purchased from Thermo Fisher Scientific (Waltham, MA, USA). PNGase F was from Roche Diagnostics (GmbH, Penzberg, Germany). Other chemicals were from Sigma-Aldrich unless otherwise specified.

Cell culture and transfections

All cell lines were maintained in Dulbecco's modified Eagle's medium supplemented with 10% fetal bovine serum (FBS; Lonza, Basel, Switzerland), at 37°C in humidity-saturated 5% CO_2 atmosphere. We generated polyclonal HeLa and HEK293 stable cell lines knockdown for TMEM165 by the shRNA technique. Cells were transfected with the pGIPZ Lentiviral shRNA plasmid (Thermo Fisher Scientific) containing either shRNA sequences targeting TMEM165 mRNA or no sequences. The selection was done with puromycine. Thus, we generated two polyclonal cell lines, named control cell line and shTMEM165 for the cell line depleted in TMEM165. For manganese treatment, $MnCl_2$ was added for the times and concentrations described in each figures.

Immunofluorescence staining

Cells were seeded on coverslips for 12–24 h, washed once in Dulbecco's phosphate-buffered saline (DPBS, Lonza) and fixed either with 4% paraformaldehyde (PAF) in phosphate-buffered saline (PBS), pH 7.3, for 30 min at room temperature or with ice-cold methanol for 10 min at room temperature. Coverslips were then washed three times with PBS. Only if the fixation had been done with PAF, cells were permeabilized with 0.5% Triton X-100 in PBS for 15 min then washed three times with PBS. Coverslips were

then put in saturation for 1 h in blocking buffer [0.2% gelatin, 2% bovin serum albumin (BSA), 2% FBS (Lonza) in PBS], followed by the incubation for 1 h with primary antibody diluted at 1:100 in blocking buffer. After washing with PBS, cells were incubated for 1 h with Alexa 488-, Alexa 568- or Alexa 700-conjugated secondary antibody (Life Technologies) diluted at 1:600 in blocking buffer. After three washing with PBS, coverslips were mounted on glass slides with Mowiol. Fluorescence was detected through an inverted Leica TCS-SP5 confocal microscope. Acquisitions were done using the LAS AF LITE software 2.6.3 (Leica Microsystem, Wetzlar, Germany).

Image analyses

Immunofluorescence images were analyzed using TisGolgi, an homemade imageJ (35) (http://imagej.nih.gov/ij, 3 February 2016, date last accessed) plugin developed by TISBio and available upon request. Basically, the program automatically detects and discriminates Golgi and vesicles, based on morphological parameters such as size and sphericity. Then, the program calculates for each image the number of detected objects, their size and mean fluorescence intensity.

PNGase F deglycosylation assay

Fifty micrograms of cell lysate are vacuum dried with SpeedVac™. Samples are then dissolved in 200 µl ammonium bicarbonate 50 mM buffer. Five microliters of a solution containing 10% SDS and 10% β-mercaptoethanol in ammonium bicarbonate 50 mM are added to the samples. Heat for 10 min at 100°C. Cool down the samples at room temperature and add 175 µl of ammonium bicarbonate 50 mM buffer. Add 25 µl of a solution containing 10% NP-40 in ammonium bicarbonate 50 mM. To perform the deglycosylation treatment, add 1,5 PNGase F unit to each sample and put the samples at 37°C overnight. Samples are then vaccum dried with SpeedVac™ and then dissolved in NuPAGE LDS sample buffer (Invitrogen) pH 8.4 supplemented with 4% β-mercaptoethanol (Fluka).

Western blotting

Cells were scraped in DPBS and then centrifuged at 4500 rpm for 3 min. Supernatant was discarded and cells were then resuspended in RIPA buffer [Tris–HCl 50 mM, pH 7.9, NaCl 120 mM, NP40 0.5%, EDTA 1 mM, Na_3VO_4 1 mM, NaF 5 mM] supplemented with a protease cocktail inhibitor (Roche Diagnostics, Penzberg, Germany). Cell lysis was done by passing the cells several times through a syringe with a 26G needle. Cells were centrifuged for 30 min at 20 000 × *g*. The supernatant containing protein was estimated with the micro BCA Protein Assay Kit (Thermo Scientific). Twenty micrograms of total protein lysate were put in NuPAGE LDS sample buffer (Invitrogen), pH 8.4, supplemented with 4% β-mercaptoethanol (Fluka). Samples were heated 10 min at 95°C and then separated on 4–12% Bis–Tris gels (Invitrogen) and transferred to nitrocellulose membrane Hybond ECL (GE Healthcare, Little Chalfont, UK). The membrane was blocked in blocking buffer (5% milk powder in TBS-T [1× TBS with 0.05% Tween 20]) for 1 h at room temperature, then incubated overnight with the primary antibodies in blocking buffer, and washed three times for 5 min in TBS-T. The membranes were then incubated with the peroxidase-conjugated secondary goat anti-rabbit or goat anti-mouse antibodies (Dako; used at a dilution of 1:10 000) in blocking buffer for 1 h at room temperature and later washed three times for 5 min in TBS-T. Signal was detected with chemiluminescence reagent (ECL 2 Western Blotting Susbtrate, Thermo Scientific) on imaging film (GE Healthcare, Little Chalfont, UK).

Glycan analysis by mass spectrometry

Cells were sonicated in extraction buffer (25 mM Tris, 150 mM NaCl, 5 mM EDTA and 1% CHAPS, pH 7.4) and then dialyzed in 6–8 kDa cut-off dialysis tubing in an ammonium bicarbonate solution (50 mM, pH 8.3) for 48 h at 4°C and lyophilized. The proteins/glycoproteins were reduced and carboxyamidomethylated followed by sequential tryptic and peptide *N*-glycosidase F digestion and Sep-Pak purification. Permethylation of the freeze-dried glycans and MALDI-TOF-MS of permethylated glycans were performed as described elsewhere (34).

Statistical analysis

Comparisons between groups were performed using Student's *t*-test for two variables with equal or different variances, depending on the result of the *F*-test.

Supplementary Material

Supplementary Material is available at *HMG* online.

Acknowledgements

We are indebted to Dr Dominique Legrand for the Research Federation FRABio (Univ. Lille, CNRS, FR 3688, FRABio, Biochimie Structurale et Fonctionnelle des Assemblages Biomoléculaires) for providing the scientific and technical environment conducive to achieving this work.

Conflict of Interest statement. None declared.

Funding

This work was supported by the French National Research Agency (SOLV-CDG to F.F.); and the Mizutani Foundation for Glycoscience, no. ANR15-CE14-0001 (to F.F.).

References

1. Scott, K., Gadomski, T., Kozicz, T. and Morava, E. (2014) Congenital disorders of glycosylation: new defects and still counting. *J. Inherit. Metab. Dis.*, **37**, 609–617.
2. Freeze, H.H. (2013) Understanding human glycosylation disorders: biochemistry leads the charge. *J. Biol. Chem.*, **288**, 6936–6945.
3. Krasnewich, D. (2014) Human glycosylation disorders. *Cancer Biomark. Sect. Dis. Markers*, **14**, 3–16.
4. Jaeken, J. (2013) Congenital disorders of glycosylation. *Handb. Clin. Neurol.*, **113**, 1737–1743.
5. Freeze, H.H. (2007) Congenital disorders of glycosylation: CDG-I, CDG-II, and beyond. *Curr. Mol. Med.*, **7**, 389–396.
6. Jaeken, J. and Matthijs, G. (2007) Congenital disorders of glycosylation: a rapidly expanding disease family. *Annu. Rev. Genomics Hum. Genet.*, **8**, 261–278.
7. Freeze, H.H., Chong, J.X., Bamshad, M.J. and Ng, B.G. (2014) Solving glycosylation disorders: fundamental approaches reveal complicated pathways. *Am. J. Hum. Genet.*, **94**, 161–175.
8. Peters, V., Penzien, J.M., Reiter, G., Körner, C., Hackler, R., Assmann, B., Fang, J., Schaefer, J.R., Hoffmann, G.F. and Heidemann, P.H. (2002) Congenital disorder of glycosylation IId (CDG-IId) – a new entity: clinical presentation with Dandy-

Walker malformation and myopathy. *Neuropediatrics*, **33**, 27–32.
9. Jaeken, J., Schachter, H., Carchon, H., De Cock, P., Coddeville, B. and Spik, G. (1994) Carbohydrate deficient glycoprotein syndrome type II: a deficiency in Golgi localised N-acetyl-glucosaminyltransferase II. *Arch. Dis. Child.*, **71**, 123–127.
10. Martinez-Duncker, I., Dupré, T., Piller, V., Piller, F., Candelier, J.-J., Trichet, C., Tchernia, G., Oriol, R. and Mollicone, R. (2005) Genetic complementation reveals a novel human congenital disorder of glycosylation of type II, due to inactivation of the Golgi CMP-sialic acid transporter. *Blood*, **105**, 2671–2676.
11. Wu, X., Steet, R.A., Bohorov, O., Bakker, J., Newell, J., Krieger, M., Spaapen, L., Kornfeld, S. and Freeze, H.H. (2004) Mutation of the COG complex subunit gene COG7 causes a lethal congenital disorder. *Nat. Med.*, **10**, 518–523.
12. Foulquier, F., Vasile, E., Schollen, E., Callewaert, N., Raemaekers, T., Quelhas, D., Jaeken, J., Mills, P., Winchester, B., Krieger, M. *et al.* (2006) Conserved oligomeric Golgi complex subunit 1 deficiency reveals a previously uncharacterized congenital disorder of glycosylation type II. *Proc. Natl. Acad. Sci. USA*, **103**, 3764–3769.
13. Kranz, C., Ng, B.G., Sun, L., Sharma, V., Eklund, E.A., Miura, Y., Ungar, D., Lupashin, V., Winkel, R.D., Cipollo, J.F. *et al.* (2007) COG8 deficiency causes new congenital disorder of glycosylation type IIh. *Hum. Mol. Genet.*, **16**, 731–741.
14. Paesold-Burda, P., Maag, C., Troxler, H., Foulquier, F., Kleinert, P., Schnabel, S., Baumgartner, M. and Hennet, T. (2009) Deficiency in COG5 causes a moderate form of congenital disorders of glycosylation. *Hum. Mol. Genet.*, **18**, 4350–4356.
15. Reynders, E., Foulquier, F., Leão Teles, E., Quelhas, D., Morelle, W., Rabouille, C., Annaert, W. and Matthijs, G. (2009) Golgi function and dysfunction in the first COG4-deficient CDG type II patient. *Hum. Mol. Genet.*, **18**, 3244–3256.
16. Kornak, U., Reynders, E., Dimopoulou, A., van Reeuwijk, J., Fischer, B., Rajab, A., Budde, B., Nürnberg, P., Foulquier, F., Lefeber, D. *et al.* (2008) Impaired glycosylation and cutis laxa caused by mutations in the vesicular H+-ATPase subunit ATP6V0A2. *Nat. Genet.*, **40**, 32–34.
17. Foulquier, F., Amyere, M., Jaeken, J., Zeevaert, R., Schollen, E., Race, V., Bammens, R., Morelle, W., Rosnoblet, C., Legrand, D. *et al.* (2012) TMEM165 deficiency causes a congenital disorder of glycosylation. *Am. J. Hum. Genet.*, **91**, 15–26.
18. Van Scherpenzeel, M., Steenbergen, G., Morava, E., Wevers, R. A. and Lefeber, D.J. High-resolution mass spectrometry glycoprofiling of intact transferrin for diagnosis and subtype identification in the congenital disorders of glycosylation. *Transl. Res.*, doi: 10.1016/j.trsl.2015.07.005.
19. Rosnoblet, C., Legrand, D., Demaegd, D., Hacine-Gherbi, H., de Bettignies, G., Bammens, R., Borrego, C., Duvet, S., Morsomme, P., Matthijs, G. *et al.* (2013) Impact of disease-causing mutations on TMEM165 subcellular localization, a recently identified protein involved in CDG-II. *Hum. Mol. Genet.*, **22**, 2914–2928.
20. Demaegd, D., Foulquier, F., Colinet, A.-S., Gremillon, L., Legrand, D., Mariot, P., Peiter, E., Van Schaftingen, E., Matthijs, G. and Morsomme, P. (2013) Newly characterized Golgi-localized family of proteins is involved in calcium and pH homeostasis in yeast and human cells. *Proc. Natl. Acad. Sci. USA*, **110**, 6859–6864.
21. Rudolph, H.K., Antebi, A., Fink, G.R., Buckley, C.M., Dorman, T. E., LeVitre, J., Davidow, L.S., Mao, J.I. and Moir, D.T. (1989) The yeast secretory pathway is perturbed by mutations in PMR1, a member of a Ca^{2+} ATPase family. *Cell*, **58**, 133–145.
22. Dürr, G., Strayle, J., Plemper, R., Elbs, S., Klee, S.K., Catty, P., Wolf, D.H. and Rudolph, H.K. (1998) The medial-Golgi ion pump Pmr1 supplies the yeast secretory pathway with Ca^{2+} and Mn^{2+} required for glycosylation, sorting, and endoplasmic reticulum-associated protein degradation. *Mol. Biol. Cell*, **9**, 1149–1162.
23. Antebi, A. and Fink, G.R. (1992) The yeast $Ca^{(2+)}$-ATPase homologue, PMR1, is required for normal Golgi function and localizes in a novel Golgi-like distribution. *Mol. Biol. Cell*, **3**, 633–654.
24. Cyert, M.S. and Philpott, C.C. (2013) Regulation of cation balance in Saccharomyces cerevisiae. *Genetics*, **193**, 677–713.
25. Dudley, A.M., Janse, D.M., Tanay, A., Shamir, R. and Church, G. M. (2005) A global view of pleiotropy and phenotypically derived gene function in yeast. *Mol. Syst. Biol.*, **1**, 2005.0001.
26. Bai, C., Xu, X.-L., Chan, F.-Y., Lee, R.T.H. and Wang, Y. (2006) MNN5 encodes an iron-regulated alpha-1,2-mannosyltransferase important for protein glycosylation, cell wall integrity, morphogenesis, and virulence in Candida albicans. *Eukaryot. Cell*, **5**, 238–247.
27. Masuda, M., Braun-sommargren, M., Crooks, D. and Smith, D. R. (2013) Golgi phosphoprotein 4 (GPP130) is a sensitive and selective cellular target of manganese exposure. *Synapse NY*, **67**, 205–215.
28. Mukhopadhyay, S., Bachert, C., Smith, D.R. and Linstedt, A.D. (2010) Manganese-induced trafficking and turnover of the cis-Golgi glycoprotein GPP130. *Mol. Biol. Cell*, **21**, 1282–1292.
29. Ca, W. and Munro, S. (1998) Activity of the yeast MNN1 alpha-1,3-mannosyltransferase requires a motif conserved in many other families of glycosyltransferases. *Proc. Natl. Acad. Sci. USA*, **95**, 7945–7950.
30. Rayner, J.C. and Munro, S. (1998) Identification of the MNN2 and MNN5 mannosyltransferases required for forming and extending the mannose branches of the outer chain mannans of Saccharomyces cerevisiae. *J. Biol. Chem.*, **273**, 26836–26843.
31. García-Rodríguez, N., Manzano-López, J., Muñoz-Bravo, M., Fernández-García, E., Muñiz, M. and Wellinger, R.E. (2015) Manganese redistribution by calcium-stimulated vesicle trafficking bypasses the need for P-type ATPase function. *J. Biol. Chem.*, **290**, 9335–9347.
32. Park, J.H., Hogrebe, M., Grüneberg, M., DuChesne, I., von der Heiden, A.L., Reunert, J., Schlingmann, K.P., Boycott, K.M., Beaulieu, C.L., Mhanni, A.A. *et al.* (2015) SLC39A8 deficiency: a disorder of manganese transport and glycosylation. *Am. J. Hum. Genet.*, **97**, 894–903.
33. Ballou, C.E.(1990) Isolation, characterization, and properties of Saccharomyces cerevisiae mnn mutants with nonconditional protein glycosylation defects. *Gene Expression Technology* (*Methods Enzymology*). Academic Press, USA, Vol. 185, pp. 440–470.
34. Morelle, W. and Michalski, J.-C. (2007) Analysis of protein glycosylation by mass spectrometry. *Nat. Protoc.*, **2**, 1585–1602.
35. Schneider, C.A., Rasband, W.S. and Eliceiri, K.W. (2012) NIH Image to ImageJ: 25 years of image analysis. *Nat. Methods*, **9**, 671–675.